SCIENTIFIC REPORTS

OPEN

SUBJECT AREAS:
ELECTRONIC PROPERTIES AND MATERIALS
SUPERCONDUCTING PROPERTIES AND MATERIALS
SPECTROSCOPY
ELECTRONIC STRUCTURE

Received
18 January 2013

Accepted
24 April 2013

Published
13 May 2013

Correspondence and requests for materials should be addressed to D.M. (dmeyers@uark.edu) or T.S.-D. (t.sahadasgupta@gmail.com)

Zhang-Rice physics and anomalous copper states in A-site ordered perovskites

D. Meyers[1], Swarnakamal Mukherjee[2], J.-G. Cheng[3,4,5], S. Middey[1], J.-S. Zhou[3], J. B. Goodenough[3], B. A. Gray[1], J. W. Freeland[6], T. Saha-Dasgupta[2] & J. Chakhalian[1,7]

[1]Department of Physics, University of Arkansas, Fayetteville, AR 72701, [2]Department of Condensed Matter Physics and Materials Science, S. N. Bose National Centre for Basic Sciences, Kolkata 700098, India, [3]Texas Materials Institute, ETC 9.102, University of Texas at Austin, Austin, Texas 78712, [4]Institute for Solid State Physics, University of Tokyo, 5-1-5 Kashiwanoha, Kashiwa, Chiba Japan 277-8581, [5]Beijing National Laboratory for Condensed Matter Physics, and Institute of Physics, Chinese Academy of Sciences, Beijing 100190, China, [6]Advanced Photon Source, Argonne National Laboratory, Argonne, Illinois 60439, USA, [7]Division of Physics and Applied Physics, School of Physical and Mathematical Sciences, Nanyang Technological University, Singapore 637 371, Singapore.

In low dimensional cuprates several interesting phenomena, including high T_c superconductivity, are deeply connected to electron correlations on Cu and the presence of the Zhang-Rice (ZR) singlet state. Here, we report on direct spectroscopic observation of the ZR state responsible for the low-energy physical properties in two isostructural A-site ordered cuprate perovskites, $CaCu_3Co_4O_{12}$ and $CaCu_3Cr_4O_{12}$ as revealed by resonant soft x-ray absorption spectroscopy on the Cu $L_{3,2}$- and O K-edges. These measurements reveal the signature of Cu in the high-energy 3+ ($3d^8$), the typical 2+ ($3d^9$), as well as features of the ZR singlet state (*i.e.*, $3d^9\underline{L}$, $\underline{L}$ denotes an oxygen hole). First principles GGA + *U* calculations affirm that the B-site cation controls the degree of Cu-O hybridization and, thus, the Cu valency. These findings introduce another avenue for the study and manipulation of cuprates, bypassing the complexities inherent to conventional chemical doping (*i.e.* disorder) that hinder the relevant physics.

The many-body ZR singlet state[1–9], a doped hole on the oxygen site coupled antiferromagnetically with a hole on the copper site, can be manipulated with conventional solid-state chemistry methods by partial removal of oxygen or by non-isovalent cation exchange (*e.g.* $La^{3+} \rightarrow Sr^{2+}$). Such chemical routes of manipulation make the the doped cuprates prone to chemical disorder causing strong structural distortions or even changes in crystal symmetry, which in turn may severely alter the properties associated with Cu *d*-electron derived electronic and magnetic structures. En route to the goal of realizing the ZR state without chemical disorder or lattice distortion, while the majority of the Cu oxide compounds have the Cu ions in the B-site of the perovskite ABO_3 structure, the A-site ordered perovskites with chemical formula $(ACu_3)B_4O_{12}$ are intriguing candidates for investigation due to the unique Cu A-site arrangement (see Fig. 1(a)). In this structure, a surprisingly rich set of interesting physics phenomena[10–16] have been demonstrated by replacement of the B-site 3*d* transition metal ion via experiment and theory including colossal dielectric constant[17,18], ferrimagnetism[19], charge, orbital, and spin ordering[20], non-fermi liquid behavior[21], enhanced electronic correlations[22] and possibly the Zhang-Rice state[23]. In addition, previous reports hinted at the presence of a mixed-valency on Cu for B = Cr and Co[23,24]. Despite the large variation in the B-site ions, all the members of this family belong to the same space group *Im*-3 built upon two sub-lattices of octahedral BO_6 units and the planar CuO_4 units (see Fig. 1(b)–(c). As seen in Fig. 1(a and d), the two structural units are connected *via* apical oxygens to form a BO_6 - CuO_4 - BO_6 cluster. In this configuration, the effect of the B-site cation has been shown to be two-fold: first, its valence state controls the nominal valence state of the A′-site Cu ion and second, most importantly, its tendency for covalent mixing alters the charge distribution between Cu d- and O p-states[11,15]. The structural similarity of the local ionic environment of Cu in these ordered perovskites with that of high T_c cuprates, and, in close analogy to chemical doping, the above-mentioned B-site's potential to engineer the electronic structure prompts one to use the A-site ordered perovskites to gain unique insight into the development of the cuprate electronic structure. Construction of such manipulated valencies suggests the ability to tune the formation of ligand holes on oxygen and possibly to achieve the formation of the Zhang-Rice singlet state - an important ingredient for high temperature superconductivity.

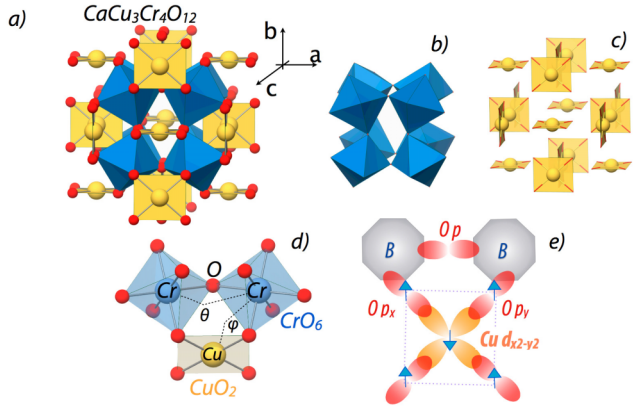

Figure 1 | Crystal structure of A-site ordered perovskites. (a) The entire crystal structure of $CaCu_3Cr_4O_{12}$. (b) CrO_6 octahedral sub-lattice. (c) CuO_4 distorted square planar sub-lattice. (d) Cr-Cr and Cr-Cu exchange pathways and (e) a sketch of B-site electronic states coupled to the ZR singlet state on Cu.

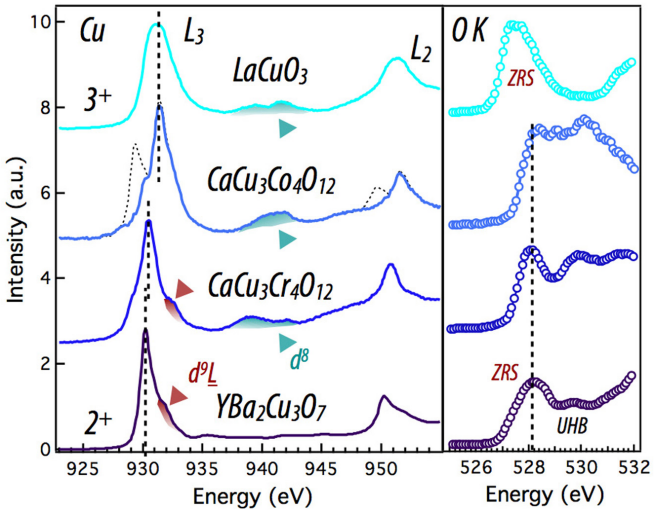

Figure 2 | XAS measurements on Cu L- and O K-edges. Left panel displays the Cu L-edge for all samples with the Zhang-Rice and d^8 ground states highlighted. LCO and YBCO are shown as references for Cu 3+ and Cu 2+ respectively, highlighting the change in valence for Cu with B-site change[36,37]. Right panel shows the corresponding O K-edge spectra displaying the Zhang-Rice ligand hole state. In LCO, the higher energy peak around ~ 940 eV is due to the presence of the unusual Cu d^8 state. In CCCoO, a previously reported impurity peak around 929 eV[32] is subtracted from both the L_3 and L_2 edges by fitting to a Voigt function. This peak corresponds to the d^9 peak observed on the other samples, however it has a very small spectral weight (~ 1/50 ratio between d^9 and $d^9\underline{L}$ states).

Results

Resonant x-ray absorption spectroscopy (XAS) in the soft X-ray regime is an ideal tool, extensively used in the past, to investigate the Cu and O electronic structure and the effects of electron-electron correlations in high T_c cuprates[2,6–8,25–27]. Results of our soft XAS measurements on the Cu $L_{3,2}$- and O K-edge are shown in Fig. 2 for the two A-site ordered perovskites $CaCu_3Co_4O_{12}$ (CCCoO) and $CaCu_3Cr_4O_{12}$ (CCCrO) along with that of the optimally doped superconducting $YBa_2Cu_3O_{7-\delta}$ (YBCO) and metallic $LaCuO_3$ (LCO) perovskite with a unique formal Cu^{3+} ($3d^8$) oxidation state. From the absorption line shape in Fig. 2, it is readily apparent that in CCCoO and CCCrO a mixed valency of Cu is present; we will discuss the CCCrO compound first. The sharp peak ~ 930 eV corresponds to the transition from the d^9 ground state, featuring a single hole in the Cu e_g band, to the $\underline{c}d^{10}$ (here $\underline{c}$ denotes a core hole) excited state. The shoulder seen at 931.5 eV, a signature of the ZR singlet state, is a transition from the ground state $d^9\underline{L}$ to the $\underline{c}d^{10}\underline{L}$ excited state[2,5,7,26,27]. The key difference between these two transitions being that while the Cu still maintains a nearly 2+ (or d^9) valency, a ligand hole is distributed over the neighboring oxygens as illustrated in Fig. 1(e). The interaction between this ligand hole and the core hole created by the photon absorption raises the energy required to promote the core electron to the unoccupied state in the e_g band resulting in the observed high-energy state marked by red arrows. Furthermore, to corroborate this, we show the absorption data on LCO with the formal Cu charge state of 3+. Indeed, in-line with our previous statement, the main feature of the LCO XAS around the L_3-edge at ~ 931.5 eV is the transition from the $d^9\underline{L}$ state, thus making the ZR state the dominant contribution to the ground state in good agreement with previous reports[28,29]. The aforementioned doped ligand holes are the charge carriers essential to the physics of high T_c cuprates; for instance, in hole doped cuprates the superconducting transition temperature is strongly dependent on the amount of doping present[2,30,31]. To clarify the connection between these compounds and the high-temperature superconducting cuprates, XAS data was taken for an optimally doped YBCO sample. As seen in Fig. 2, the Cu L-edge spectrum of CCCrO shows remarkable resemblance to YBCO, namely the dominant d^9 initial states followed by the higher energy ZR state shoulder. This result highlights the capacity of the A-site ordered cuprate perovskites to *mimic the effects of chemical doping* without provoking unwanted lattice and stoichiometry deviations inherent to conventional chemical doping. In addition, the multiplet split peak at ~ 940 eV corresponds to a transition from the metastable $3d^8$ state to the cd^9 excited state, indicating the presence of the ionically Cu^{3+} state entirely absent in YBCO.

Next, we turn our attention to the CCCoO electronic structure. As clearly seen in Fig. 2, CCCoO shows a dominant white absorption line analogous to CCCrO, but, surprisingly, it is shifted ~ 1 eV away from the d^9 white line of CCCrO and YBCO. When compared with the formally Cu^{3+} compound LCO (shown immediately above it in Fig. 2) it becomes readily apparent that the Cu ground state is predominantly of $d^9\underline{L}$ character, implying a dominant Cu^{3+} formal valence as in LCO. To quantify the prevalence of the $d^9\underline{L}$ state, a three peak fit is used for the L_3 data, which are centered at 929.3 eV (impurity)[32], 930 eV (d^9), and 931.4 eV ($d^9\underline{L}$) which gave a very small spectral weight ratio of .0203 $\left(\frac{d^9}{d^9\underline{L}}\right)$. The impurity peak was subtracted from the original data (dotted line) for clarity. Further demonstrating the 3+ formal valence, the multiplet split peak at ~940 eV provides strong evidence for the admixture of the d^8 state. When considered alongside CCCrO, CCCoO also contains all three Cu states, but with obviously significantly different weights, further testifying to the ability of the B-site to effectively hole dope the Cu sites.

Because of the large degree of charge transfer between oxygen and copper and its importance to the ZR state, studies of the O K-edge can lend supporting information about the electronic structure of Cu. As seen in Fig. 2(b), O K-edge data in all samples show the oxygen specific signature of the $3d^9\underline{L}$ state, a necessary ingredient of the ZR state, which is particularly evident from the comparison to the well studied case of YBCO, where the ligand hole on oxygen appears as a large, doping dependent pre-peak around 528 eV[6–8,25]. This observation of the pre-peak intensity indicates that the ZR state is the first ionization state at the Fermi energy. This further evidences our conclusion on the presence of the ZR state inferred from the Cu L-edge analysis.

Although our prime focus is on the electronic structure of Cu and O, Co and Cr $L_{3,2}$-edge absorption can serve to independently

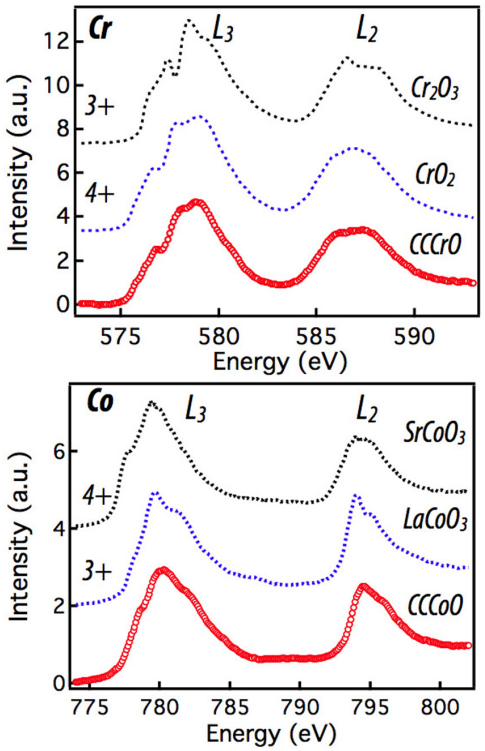

Figure 3 | XAS measurements on the Cr and Co L-edges. (a) The Cr L-edge along with 3+ and 4+ references from[33], the CCCrO and the 4+ reference samples show strong similarities. (b) The Co L-edge with valence references from[34] showing a similar, but not identical line shape. No standards were available meaning any energy shift between the samples could not be analyzed, all spectra were shifted to ~ align the white lines.

validate the Cu oxidation state. With this goal in mind, we performed L-edge XAS measurements on Co and Cr and compared this to the previous results on reference Cr and Co compounds. As shown in Fig. 3(a), a direct comparison to the Cr^{3+} and Cr^{4+} absorption confirms that in CCCrO the Cr valency is 4+ or very close to it[33]. This verifies the conclusion that, in this compound, if Cr is 4+ then Cu must be ~2+ (assuming O^{2-} and Ca^{2+}). Any deviation of Cr valency towards 3+ must then be compensated by raising the Cu charge state, thus Cu must be 2 + or very close to it, consistent with the Cu L-edge results. The Co L-edge data shown in Fig. 3(b) bear strong similarities with previous studies of $LaCoO_3$, which consists of ionically bound Co^{3+}[34]. Specifically, strong, high energy multiplet shoulders on the L_3 and L_2 white lines are present in both CCCoO and $LaCoO_3$. In variance to this, Co^{4+} shows a smaller shoulder shifted to even higher energy. While the high energy side of the CCCoO Co L-edge is consistent with Co^{3+}, the low energy multiplet peak does not match either 3+ or 4+, implying CCCoO is neither ionically pure 3+ or 4+. Based upon the Cu L-edge conclusion of the Cu^{3+} charge state, we can independently assess the Co valency to be ~ 3.25+. In this context, the Co L-edge data is compatible with the Cu L-edge results and implies the presence of a mixed 3+/4+ Co valency, although it cannot confirm the exact 3.25+ valence state needed to conserve charge. Lending further support to this conclusion, Co L edge data in total electron yield (TEY) mode is shown in the Supplemental Figure S1.

To gain further understanding of the B-site influence on the unusual electronic states on Cu, we performed first-principles spin-polarized DFT calculations within the GGA+*U* approximation. Fig. 4 summarizes the first-principles results for CCCoO and CCCrO, respectively. Note, although no long-range magnetic ordering is reported in these compounds, spin-polarized calculations are

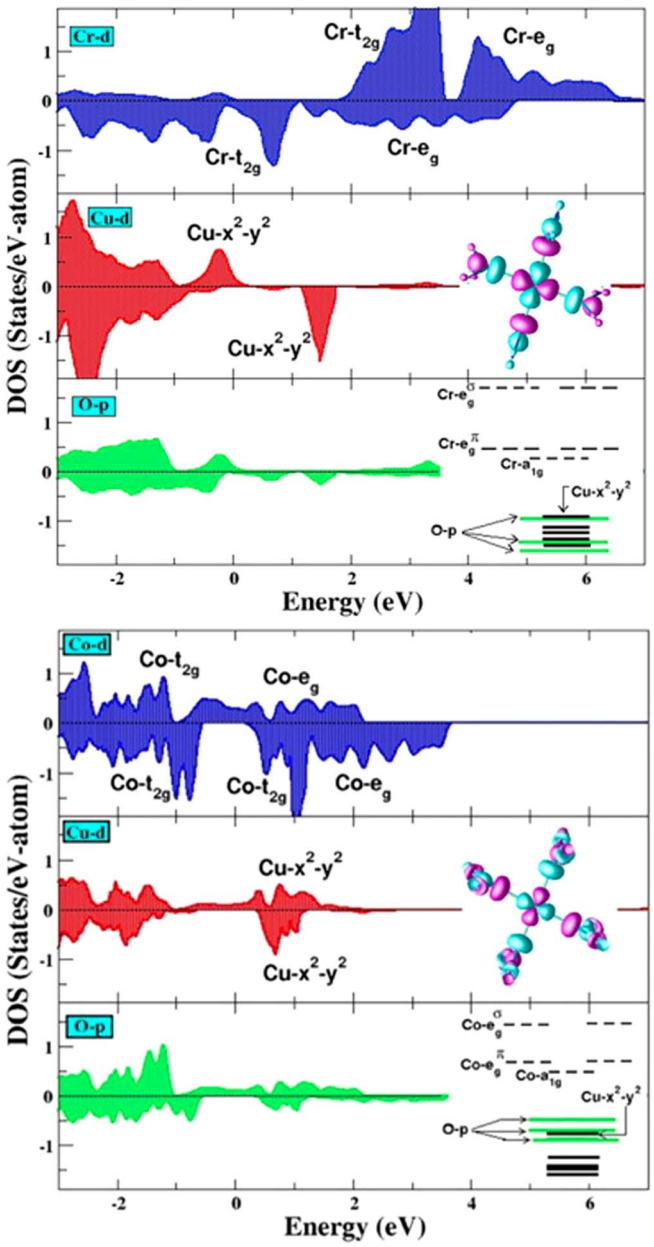

Figure 4 | The GGA + *U* density of states, projected onto Co d (Cr d), Cu d and O p states for the A-site ordered perovskites. (a) $CaCu_3Co_4O_{12}$ ((b) $CaCu_3Cr_4O_{12}$) compound. The positive and negative values in y-axis correspond to density of states inup and down spin channels, respectively. The zero of the energy is set at E_F. The features due to dominant contributions of various degrees of freedom have been marked. The inset in the middle panel shows the plot of the effective Cu $x^2 - y^2$ Wannier function, calculated by NMTO-downfolding. Shown are the isosurface with lobes of opposite signs are colored differently. The inset in the bottom panel shows the relative positions of Co d, Cu d and O p energy levels.

essential for proper assignment of both charge and spin states of various constituents[15]. The three panel Fig. 4(a) and (b) show an inspection of the calculated density of states (DOS) projected onto B-d (B=Co/Cr), Cu-d and O-p states respectively. A direct inspection of the states in the vicinity to the Fermi energy, E_F demonstrates the existence of strong mixing between B and Cu d-states and O p-states. This strong covalency effect makes both CCCoO and CCCrO systems metallic, in agreement with experimental observations. In addition, as shown in the inset of Fig. 4(a)–(b), the octahedral crystal field

of the oxygen atoms around the B ion splits the B-t_{2g} states from the B-e_g $\left(e_g^{\sigma}\right)$ states; the trigonal distortion present in the BO_6 octahedra breaks the t_{2g} levels further into doubly degenerate, e_g^{π} and singly degenerate a_{1g} states. The distorted square planar environment of oxygen atoms surrounding the Cu ion, on the other hand, lifts the 5-fold degeneracy of Cu d-levels, with large energy separation of Cu $d_{x^2-y^2}$ state from the rest. Here we note that the nominal d^8 (*i.e.* Cu^{3+}) would imply empty Cu: $d_{x^2-y^2}$ states in both spin up and spin down channels, and for d^9 Cu : $d_{x^2-y^2}$ states would be occupied in one of the spin channels and be empty in the other spin channel. From the DOS plots shown in Fig. 4(a) and (b), we find that Cu: $d_{x^2-y^2}$ states are empty in the down spin channel, while in the up spin channel it is indeed close to being empty for CCCoO, but mostly occupied for CCCrO. We note that DFT calculation deals with single configuration nature of the wavefunction and therefore, delivers the state with most dominant weight. Interestingly enough, the dominance of Cu 3+ state in CCCoO and Cu 2+ state in CCCrO is evident even at the level of single configuration theory. This result lends strong theoretical support for the conclusion inferred from our XAS measurements that the Cu state is predominantly in the 3+ state for CCCoO and closer to 2+ for CCCrO.

Next, we discuss the calculated magnetic states in connection to Cu. First, we note that occupancy of the square planar Cu d-states according to the formal valence of d^8 would give rise to a paired electronic configuration with zero magnetic moment at Cu sites, while that of formal valence of d^9 would give rise to one unpaired electron with magnetic moment of 1 μ_B in the fully spin polarized limit. In comparison, the calculation yields magnetic moments on Cu site 0.07 μ_B for CCCoO and 0.50 μ_B for CCCrO, thus lending additional validation of our experimental conclusion on the exotic 3+ state for CCCoO and closer to 2+ valency in CCCrO. Moreover, from the simple ionic charge count, the nominal 3+ and 2+ valences of Cu (assuming Ca^{2+} and O^{2-}), would set the formal valences of the B-site ion to 3.25+ and 4+ respectively, and result in d-electron occupancies of 5.75 for Co and 2 for Cr. The computed magnetic moment at the Cr site is 2.2 μ_B, in good agreement with the nearly 2+ valence of Cu and 4+ valence of Cr in CCCrO. The d-occupancy of 5.75 on Co can lead to either low or high spin magnetic state; our computed Co magnetic moment of $\sim$1.7 μ_B, however, is in conformity with the intermediate rather than low- or high-spin state.

By examining the energy level positions, as calculated in DFT, shown in the insets in the bottom panels of Figs. 4(a–b), we find that Cu $d_{x^2-y^2}$ energy level is nearly degenerate with O-*p* states, leading to a situation very similar to that in high T_c cuprates. This electronic configuration naturally supports strong mixing of Cu $d_{x^2-y^2}$ and O p_x and p_y states by forming a strong pdσ antibonding combination, which may further bind to d-states at the B site as shown in Fig. 1(e). The formation of such a mixed state is also evident in the Wannier function plot of an effective Cu $x^2 - y^2$ Wannier function obtained by keeping only Cu $d_{x^2-y^2}$ state active and downfolding or integrating out all the other degrees of freedom (see inset of the middle panel of Fig. 4). We notice that for the Co compound mixing of Cu-O hybridized states with B-site d-states is much stronger compared to that of Cr compound, which is driven by the strong hybridization of empty $Cu_{x^2-y^2}$ orbital of Cu 3+ state with empty Co, e_g orbitals. In CCCrO, this leads to vanishing contribution of the B-site states for the selected iso-surface value of the Wannier plot, showing the typical Cu-O antibonding wavefunction, making the situation more like high T_c cuprates with dominant Cu 2+ state. The strong mixing between $Cu_{x^2-y^2}$ and O p states, which is a prerequisite for formation of the ZR state - observed as the feature around 931 eV in Cu L-edge spectra, is further corroborated by the presence of a 0.2 μ_B fraction of the magnetic moment on the O site and 0.5 μ_B on Cu. We thus conclude that the formation of a ZR like many-body state similar to what is observed on the high T_c cuprates is indeed highly favorable in these systems with enhanced probability for the Cr compound.

Discussion

In summary, resonant soft X-ray absorption data on Cu $L_{3,2}$- and O K-edges revealed the presence of the ZR singlet state in the symmetrically invariant A-site-ordered cuprate compounds, $CaCu_3Co_4O_{12}$ and $CaCu_3Cr_4O_{12}$. Additionally, the data demonstrated the existence of a mixed valency for Cu modulated by the electronic state of the B-site cation and reflected in the d^9, $d^9\underline{L}$, and the metastable d^8 states of Cu d-electrons. First principles GG$\bar{A}$ + *U* calculations further validate the notion that within the A-site ordered perovskite family, the choice of B-site cation is an effective tool to manipulate the degree of B-Cu-O hybridization, adjusting the Cu valency towards the unusual 3+ valence state in CCCoO and away from 3+ closer to the stable 2+ valency in CCCrO. Additionally, Wannier function calculations support this direct experimental observation that in the CCCrO compound the ZR many-body state is particularly favorable and controls the low-energy physics. These findings demonstrate that the charge and spin state of Cu, fundamental to the intriguing physical properties the cuprates display, can be effectively altered by a careful choice of the B-site cation on isomorphic lattices that circumvent the chemical disorder and lattice modulation intrinsic to other doping methods.

Methods

Experimental details. Polycrystalline $CaCu_3B_4O_{12}$ (B = Cr and Co) samples were prepared under high-pressure and high-temperature (HPHT) conditions with a Walker-type multianvil module (Rockland Research Co.). For B = Cr, stoichiometric amounts of CaO, CuO, and CrO_2 powders were thoroughly mixed and then subjected to a HPHT treatment at 7 GPa and 900°C for 30 minutes. For B = Co, a precursor containing Ca, Cu, and Co ions in the 1 : 3 : 4 molar ratio obtained via a sol-gel route was mixed with 30 wt.% $KClO_4$ acting as an oxidizing agent and then subjected to a HPHT treatment at 9 GPa and 1000°C for 30 minutes. The resultant KCl was washed away with deionized water. Details about the sample assembly and procedures for the HPHT experiment can be found in a previous paper[35]. Phase purity of the above samples was examined with powder X-ray diffraction (XRD) at room temperature with a Philips Xpert diffractometer (Cu Kα radiation). The B = Co sample contains a small amount of cobalt and copper oxides. The cubic lattice parameter was calculated to be a = 7.2385(5) and 7.1259(3) Å for M = Cr and Co, respectively. Reitveld refinement for the two a-site ordered compounds is available in the Supplemental Figure S2.

LCO was synthesized under high oxygen pressure to the rhombohedral symmetry, details of which can be found elsewhere[36]. YBCO was grown with pulsed laser deposition, the details of which can also be found elsewhere[37].

In order to elucidate the transformation of the Cu valency across these compounds, soft XAS measurements were carried out at the soft x-ray branch at the 4-ID-C beamline in the bulk-sensitive total fluorescence yield (TFY) mode and TEY mode in the Advanced Photon Source at Argonne National Laboratory. Measurements were taken on the Cu L-edge and O-K edge for all samples. All measurements were accompanied by a CuO standard, which allows precise alignment of the energy for oxidation state comparison. The Co and Cr L-edges were also obtained for the corresponding samples. All measurements shown were obtained in TFY mode; except, the Cr L edge data and all the Cr reference absorption data were taken in TEY mode.

Computational details. In the first-principles DFT calculations we have used the plane wave basis set and pseudo-potentials as implemented in the Vienna Ab-initio Simulation Package (VASP)[38]. The exchange-correlation function was chosen to be that of generalized gradient approximation (GGA) implemented following the parametrization of Perdew-Burke-Ernzerhof[39]. The electron-electron correlation beyond GGA was taken into account through improved treatment of GGA + *U* calculation within the +*U* implementation of Dudarev *et al.*[40]. For the plane wave based calculations, we used projector augmented wave (PAW)[41] potentials. The wave functions were expanded in the plane wave basis with a kinetic energy cutoff of 600 eV and Brillouin zone summations were carried out with a 6 × 6 × 6 k-mesh. The *U* value of 5 eV on Cu site and 4 eV on B site were used for GGA + *U* calculations while the Hund's rule coupling *J* was fixed to 0.8 eV. The obtained results were verified in terms of variation of *U* parameter.

In order to estimate the positions of the Cu-d, B-d and O-p energy levels as well as the plots of the effective Wannier functions for B-d states, we used muffin-tin orbital (MTO) based N-th order MTO (NMTO)[42]-downfolding calculations. Starting from a full DFT calculations, NMTO-downfolding arrives at a few-orbital Hamiltonian by integrating out degrees which are not of interest. It does so by

defining energy-selected, effective orbitals which serve as Wannier-like orbitals defining the few-orbital Hamiltonian in the *downfolded* representation. NMTO technique which is not yet available in its self-consistent form relies on the self-consistent potential parameters obtained out of linear muffin-tine orbital (LMTO)[43] calculations. The results were cross-checked among the plane wave and LMTO calculations in terms of total energy differences, density of states and band structures.

1. Zaanen, J., Sawatzky, G. A. & Allen, J. W. Band gaps and electronic structure of transition-metal compounds. *Phys. Rev. Lett.* **55**, 418 (1985).
2. Plakida, Nikolay. *High-Temperature Cuprate Superconductors.* Berlin: Springer-Verlag, 2010.
3. Chakhalian, J. *et al.* Orbital Reconstruction and covalent bonding at an oxide interface. *Science* **318**, 1114–1117 (2007).
4. Chakhalian, J. *et al.* Magnetism at the interface between ferromagnetic and superconducting oxides. *Nat. Phys.* **2**, 244–8 (2006).
5. Karpinen, M & Yamauchi, H. The doping routes and distribution of holes in layered cuprates: a novel bond-valence approach. *Phil. Mag. B* **79**, 2, 343–66 (1999).
6. Nücker, N., Fink, J., Fuggle, J. C., Durham, P. J. & Temmerman, W. M. Evidence for holes on oxygen sites in the high T_c superconductors $La_{2-x}Sr_xCuO_4$ and $YBa_2Cu_3O_{7-\gamma}$. *Phys. Rev. B* **37**, 10 (1988).
7. Nücker, N. *et al.* Site-specific and doping-dependent electronic structure of $YBa_2Cu_3O_x$ probed by O1s and Cu 2p x-ray-absorption spectroscopy. *Phys. Rev. B* **51**, 13 (1995).
8. Kuiper, P. *et al.* X-ray absorption study of the O 2p hole concentration dependence on O stoichiometry in $YBa_2Cu_3O_x$. *Phys. Rev. B* **38**, 10 (1988).
9. Zhang, F. C. & Rice, T. M. Effective hamiltonian for the superconducting Cu oxides. *Phys. Rev. B* **37**, 3759–3761 (1988).
10. Xiang, H. P., Liu, X. J., Meng, J. & Wu, Z. J. Structural stability and magnetic coupling in $CaCu_3Co_4O_{12}$ from first principles. *J. Phys.: Condens Matter* **21**, 045501 (2009).
11. Shimakawa, Y. A-site-ordered perovskites with intriguing physical properties. *Inorg. Chem* **47**, 8562–70 (2008).
12. Alippi, P. & Fiorentini, V. Magnetism and unusual Cu valency in quadruple perovskites. *Eur, Phys. J. B.* **85**, 82 (2012).
13. Tran, T. T., Takubo, K., Mizokawa, T., Kobayashi, W. & Terasaki, I. Electronic structure of $CaCu_3Ru_4O_{12}$ studied by x-ray photoemission spectroscopy. *Phys. Rev. B* **73**, 193105 (2006).
14. Shiraki, H., Saito, T., Azuma, M. & Shimakawa, Y. Metallic behavior n A-site-ordered perovskites $ACu_3V_4O_{12}$ with A = Na^+, Ca^{2+}, and Y^{3+}. *J. Phys. Soc. Jpn.* **77**, 6 (2008).
15. Mukherjee, S., Sarkar, S. & Saha-Dasgupta, T. First Principles study of $CaCu_3B_4O_{12}$ (B=Co, Rh, Ir). *J. Mater. Sci.* **47**, 7660–4 (2012).
16. Long, Y. W. *et al.* Temperature-induced A-B intersite charge transfer in a A-site-ordered $LaCu_3Fe_4O_{12}$ perovskite. *Nature* **458**, 60 (2009).
17. McGuinness, C. *et al.* X-ray spectroscopic study of the electronic structure of the high-dielectric-constant material $CaCu_3Ti_4O_{12}$. *Phys. Rev. B* **71**, 19511 (2005).
18. Lin, Y., Chen, Y. B., Garret, T., Liu, S. W. & Chen, C. L. Epitaxial growth of dielectric $CaCu_3Ti_4O_{12}$ thin films on (001) $LaAlO_3$ by pulsed laser deposition. *Appl. Phys. Lett.* **81**, 631–3 (2002).
19. Yamada, I. *et al.* A perovskite containing quadrivalent iron as a charge-disproportionated ferrimagnet. *Angew. Chem. Int. Ed* **47**, 7032–5 (2008).
20. Prodi, A. *et al.* Charge, orbital and spin ordering phenomena in the mixed valence manganite $(NaMn^{3+}{}_3)(Mn^{3+}{}_2Mn^{4+}{}_2)O_{12}$. *Nat. Mater.* **3**, 48–52 (2004).
21. Tanaka, S., Shimazui, N., Takatsu, H., Yonezawa, S. & Maeno, Y. Heavy-Mass Behavior of Ordered Perovskites $ACu_3Ru_4O_{12}$ (A=Na, Ca, La). *J. Phys. Soc. Jpn.* **78**, 024706 (2009).
22. Hollmann, N. *et al.* Correlation effects in CaCu3Ru4O12 arXiv: 1211.2984v1.
23. Mizokawa, T. *et al.* Metallic versus insulating behavior in the A-site ordered perovskite oxides $ACu_3Co_4O_{12}$ (A=Ca and Y) controlled by Mott and Zhang-Rice physics. *Phys. Rev. B* **80**, 125105 (2009).
24. Subramanian, M. A., Marshall, W. J., Calvarese, T. G. & Sleight, A. W. Valence degeneracy in $CaCu_3Cr_4O_{12}$. *J. Phys. and Chem. Solids* **64**, 1569–71 (2003).
25. Chen, C. T. *et al.* Electronic States in $La_{2-x}Sr_xCuO_{4+\delta}$ probed by soft-x-ray absorption. *Phys. Rev. Lett.* **66**, 1 (1991).
26. Grioni, M. *et al.* Studies of copper valence states with Cu L_3 x-ray absorption spectroscopy. *Phys. Rev. B* **39**, 3 (1989).
27. Bianconi, A. *et al.* Linearly polarized Cu L_3-edge x-ray-absorption near-edge structure of $Bi_2CaSr_2Cu_2O_8$. *Phys. Rev. B* **44**, 18 (1991).
28. Mizokawa, T., Fujimori, A., Namatame, H., Takeda, Y. & Takano, M. Electronic structure of tetragonal $LaCuO_3$ studied by photoemission and x-ray-absorption spectroscopy. *Phys. Rev. B* **57**, 16 (1998).
29. Sarangi, R. *et al.* X-ray absorption edge spectroscopy and computational studies on $LCuO_2$ species. *J. Am. Chem. Soc.* **128**, 8286–96 (2006).
30. LeBoeuf, D. *et al.* Electron pockets in the Fermi surface of hole-doped high-T_c superconductors. *Nature* **450**, 533–6 (2007).
31. Ando, Y., Komiya, S., Segawa, K., Ono, S. & Kurita, Y. Electronic phase diagram of high-T_c cuprate superconductors from a mapping of the in-plane resistivity curvature. *Phys. Rev. Lett.* **93**, 267001 (2004).
32. Sarma, D. D. *et al.* Electronic structure of high-T_c superconductors from soft-x-ray absorption. *Phys. Rev. B* **37**, 16 (1988).
33. Debkov, Y. S. *et al.* Correlations in the electronic structure of half-metallic ferromagnetic CrO_2 films: An x-ray absorption and resonant photoemission spectroscopy study. *Phys. Rev. B* **72**, 060401(R) (2005).
34. Medling, S. *et al.* Evolution of magnetic oxygen states in Sr-doped $LaCoO_3$. *Phys. Rev. Lett.* **109**, 157204 (2012).
35. Cheng, J.-G., Zhou, J.-S. & Goodenough, J. B. Evolution of ferromagnetism in orthorhombic perovskites $Sr_{1-x}Pb_xRuO_3$. *Phys. Rev. B* **81**, 134412 (2010).
36. Zhou, J.-S., Archibald, W. & Goodenough, J. B. Approach to Curie-Weiss paramagnetism in the metallic perovskites $La_{1-x}Nd_xCuO_3$. *Phys. Rev. B* **61**, 3196–3199 (2000).
37. Gray, B. A. *et al.* arXiv:1301.3736.
38. Kresse, G. & Furthmuller, J. Efficient iterative schemes for ab initio total-energy calculations using a plane-wave basis set. *Phys. Rev. B* **54**, 11169 (1996).
39. P. Perdew, J., Burke, K. & Ernzerhof, M. Generalized Gradient Approximation Made Simple. *Phys. Rev. Lett.* **77**, 3865 (1996).
40. Dudarev, S. L., Botton, G. A., Savrasov, S. Y., Humphreys, C. J., & Sutton, A. P. Electron-energy-loss spectra and the structural stability of nickel oxide: An LSDA + U study. *Phys. Rev. B* **57**, 1505 (1998).
41. Blöchl, P. E. Projector augmented-wave method. *Phys. Rev. B* **50**, 17953 (1994).
42. Andersen, O. K. & Saha-Dasgupta, T. Muffin-tin orbitals of arbitrary order. *Phys. Rev. B* **62**, R16219 (2000).
43. Andersen, O. K. & Jepsen, O. Explicit, First-Principles Tight-Binding Theory. *Phys. Rev. Lett.* **53**, 2571 (1984).

Acknowledgements

JC is supported by DOD-ARO Grant No. 0402-17291. JSZ and JBG is supported by NSF Grant. No. DMR-1122603. TS-D would also like to thank, CSIR and DST, India for funding. Work at the Advanced Photon Source, Argonne is supported by the U.S. Department of Energy, Office of Science under Grant No. DEAC02-06CH11357. Thanks to Dr. Bogdan Dabrowski for the $SrCoO_{2.9}$ (~4+) sample. JGC acknowledges the support from the Japan Society for the Promotion of Science (Grant No. 12F02023) and the Chinese Academy of Sciences.

Author contributions

D.M., J.W.F. and J.C. acquired the experimental data. S.M. and T.S.-D. did the theoretical calculations. J.G.C., J.S.Z. and J.B.G. grew the samples. S.M. and B.A.G. analyzed data and provided notes on the initial versions of the manuscript. D.M., T.S.-D. and J.C. wrote the final version of the manuscript.

Additional information

Supplementary information accompanies this paper at http://www.nature.com/scientificreports

Competing financial interests: The authors declare no competing financial interests.

How to cite this article: Meyers, D. *et al.* Zhang-Rice physics and anomalous copper states in A-site ordered perovskites. *Sci. Rep.* **3**, 1834; DOI:10.1038/srep01834 (2013).